Clusters in intense FLASH pulses: ultrafast ionization dynamics and electron emission studied with spectroscopic and scattering techniques

2010 J. Phys. B: At. Mol. Opt. Phys. 43 194011

(http://iopscience.iop.org/0953-4075/43/19/194011)

J. Phys. B: At. Mol. Opt. Phys. **43** (2010) 194011 (11pp) doi:10.1088/0953-4075/43/19/194011

Clusters in intense FLASH pulses: ultrafast ionization dynamics and electron emission studied with spectroscopic and scattering techniques

C Bostedt[1,3], M Adolph[1], E Eremina[1], M Hoener[1,4], D Rupp[1], S Schorb[1], H Thomas[1,5], A R B de Castro[2] and T Möller[1]

[1] Institut für Optik und Atomare Physik, Technische Universität Berlin, Berlin, Germany
[2] IFGW UNICAMP, Campinas SP Brazil and Brazilian Synchrotron Source LNLS, Campinas SP, Brazil

E-mail: Bostedt@slac.stanford.edu and thomas.moeller@physik.tu-berlin.de

Received 16 March 2010, in final form 19 July 2010
Published 10 September 2010
Online at stacks.iop.org/JPhysB/43/194011

Abstract
FLASH, the first FEL operating at short wavelength, has paved the way for novel types of experiments in many different scientific disciplines. Key questions for the first experiments with this new type of light source are linked to light–matter interaction and ionization processes. This paper gives an overview of the ultrafast ionization dynamics and electron emission of pure and doped rare gas clusters illuminated with intense short-wavelength pulses by summarizing the findings of recent years' work at FLASH. Atomic clusters are ideal for investigating the light–matter interaction because their size can be tuned from the molecular to the bulk regime, thus allowing us to distinguish between intra and interatomic processes. The ionization processes turned out to be strongly wavelength dependent. Plasma absorption, while dominant at 13 eV, becomes insignificant at photon energies above 40 eV. The cluster ionization and disintegration proceed in several steps on a time scale from fs to ps. Insight into the involved processes can be obtained with ion and electron spectroscopy. The high intensity of FLASH pulses opens the door for a new imaging approach to study nanoparticles. Scattering patterns of single and few clusters can be recorded in a single shot. Initial results of scattering experiments and their comparison to Mie calculations show that two- and three-dimensional structural information of gas phase particles can be obtained this way.

(Some figures in this article are in colour only in the electronic version)

1. Introduction

Short-wavelength FELs, especially FLASH [1] at DESY as the first source of this new type, have opened the door to novel types of experiments in many different disciplines, ranging from nonlinear processes in atoms and molecules to ultrafast processes in condensed matter and plasma physics [2]. Experiments at FLASH started in 2001 with a study on the ultrafast ionization dynamics of clusters [3]. A key question for the first experiments with intense short-wavelength pulses concerns light–matter interaction. Understanding the interaction of light with matter has been a central theme of physics over the past century, starting with the concept of the photon and the inception of quantum theory. The continuing advance in laser technology has made it possible to explore regimes of nonlinear light–matter interaction. With FEL-type sources such as FLASH, we are now witnessing the discovery of new light-induced processes in the soft x-ray regime.

One of the most exciting prospects of research with x-ray lasers is direct imaging of nonperiodic nanoscale objects, such

[3] Present address: Linac Coherent Light Source, SLAC National Accelerator Laboratory, 2575 Sand Hill Road, Menlo Park, CA 94025, USA.
[4] Present address: Department of Physics, Western Michigan University, Kalamazoo, MI, 49008, USA.
[5] Present address: Department of Physics, University of Texas at Austin, Austin, TX 78712, USA.

as large molecules, nanocrystals, biomolecules, living cells and viruses. Understanding the interaction of intense x-ray pulses with atomic and molecular systems and the underlying physical processes is crucial for the success of these imaging experiments. For the experimental investigation of matter in intense light pulses atomic clusters are ideal because their size can be tuned from the molecular to the bulk regime and there is no energy dissipation into the surrounding media. As we will see, the ionization dynamics of clusters in intense laser pulses depends considerably on the radiation wavelength. Work with intense infrared (IR) lasers was started in the 1990s (see for example [4]). In the IR spectral regime, a transient nanoplasma is created *(inner ionization)* [5] which is then efficiently heated by inverse Bremsstrahlung (IBS) and resonant plasmon excitations leading to removal of the electrons (*outer ionization*) [6, 7], finally resulting in Coulomb explosion of the cluster. Because heating by IBS scales with $\lambda^{8/3}$ [8, 9], it was a big surprise when the first experiments at FLASH at 100 nm wavelength reported unexpectedly high energy absorption and a complete Coulomb explosion at a power density of 10^{13} W cm^{-2} [3]. Shortly after the first experiments, it became possible to extend the studies to shorter wavelength [10] and ultimately allowing ionization of inner shell electrons [11, 12]. The present research on clusters in intense FEL beams focuses on the following issues.

- What are the dominant ionization processes?
- Which atomic charge states are formed *inside* highly charged clusters?
- How does the removal of innershell electrons affect the electron dynamics and photo absorption?
- What is the effect of secondary electrons, e.g. Auger electrons?
- How does the chemical composition affect the ultrafast dynamics (non-metal/metal)?
- What is the time scale of electron removal (valence/innershell) from the cluster atoms?
- Finally, can Coulomb explosion be delayed by a tamper?

The last two points are especially interesting in view of the imaging of nanoparticles. Generation of unbound electrons inside the cluster results in the reduction of the contrast and thus hinders imaging.

This paper gives an overview of the achievements at FLASH during the first years of operation. After an experimental section, the results of ion and electron dynamics in highly excited clusters obtained with spectroscopic techniques are reviewed. Finally, first results of single-shot scattering experiments with single clusters are presented.

2. Experimental details

The experiments are performed at the FLASH free electron laser in Hamburg [1] at photon energies between 13 and 90.5 eV. In the single bunch operation mode FLASH typically delivers average pulse energies of 50 μJ and pulse durations of about 20 fs [13]. The photon beam is focused either with the ellipsoidal beamline mirror under grazing incidence down to a spot size of 20 μm full width at half maximum (FWHM) [14] or with a multilayer mirror to a focal spot of 5–10 μm FWHM resulting in peak intensities up to a few 10^{15} W cm^{-2}.

The clusters are produced by expanding pure or mixed rare gases through a cryogenically cooled, pulsed nozzle, either with a diameter of the opening cone of 100 μm (half opening angle 15°) or with 200 μm diameter and 4° half opening cone angle. The cluster beam is heavily diluted with a double-skimmer setup to avoid space charge effects in the interaction region. For the spectroscopy experiments, the average cluster size is derived from scaling laws [15, 16]. For some experiments, Xe core–Ar shell clusters are prepared. In this case their size and composition are derived from empirical laws obtained in early work on mixed clusters [11, 17–19]. For the imaging experiments, very large clusters are prepared by expanding a gas mixture of 5% Xe in Ar at 120 K and up to 8 bar total pressure. Under these conditions, the Xe partial pressure is several times higher than the vapour pressure at 120 K and to the best of our knowledge scaling laws do not exist for these extreme expansion conditions. To pick single clusters, an additional piezo-driven slit assembly is mounted directly in front of the interaction region, which was tuned so that on average less than one cluster is in the focal volume.

For electron and ion detection, time-of-flight (tof)-type spectrometers are used. For ion detection, the tof is usually operated with 1.5 kV acceleration voltage. The electron spectrometer is field free and mounted perpendicular to the laser polarization plane to increase the signal contrast between the atom and cluster contributions [10]. Due to the apertures in the spectrometer, the electron detection is limited to a few percent of the full solid angle.

For the investigation of x-ray scattering from single nanoclusters, we have developed a high repetition rate scattering detector (see figure 1) for use at short-wavelength free electron laser sources. It is based on a multi-channel plate (MCP) in combination with a phosphorous screen as photon amplifier and an out of vacuum CCD camera. The MCP front is pulsed active with a negative voltage for only 50 ns during the arrival of the light pulse. In this way, photoelectrons generated by the laser pulse are deflected from the detector and the MCP is switched off prior to the arrival of ionic fragments from the nanoclusters explosion, resulting in clean scatter photon detection. The x-ray pulse can exit through a 3 mm hole in the detector assembly. This setup allows the detection of scattering angles from $\pm$ 3° to 50° over 2π covering a large solid angle. The experiments were performed with intense soft x-ray pulses at $\lambda = 13.7$ nm and pulse length of 10–20 fs resulting in power densities up to 5×10^{13} W cm^{-2}. All data are stored shot by shot with a unique pulse identifier so that it can be correlated to the laser parameters in the post analysis.

3. Results

3.1. Ionization, light absorption and fragmentation studied with ion spectroscopy

In the first study [3] on gas phase targets at FLASH, Xe atoms and clusters were irradiated with intense pulses at 13 eV with

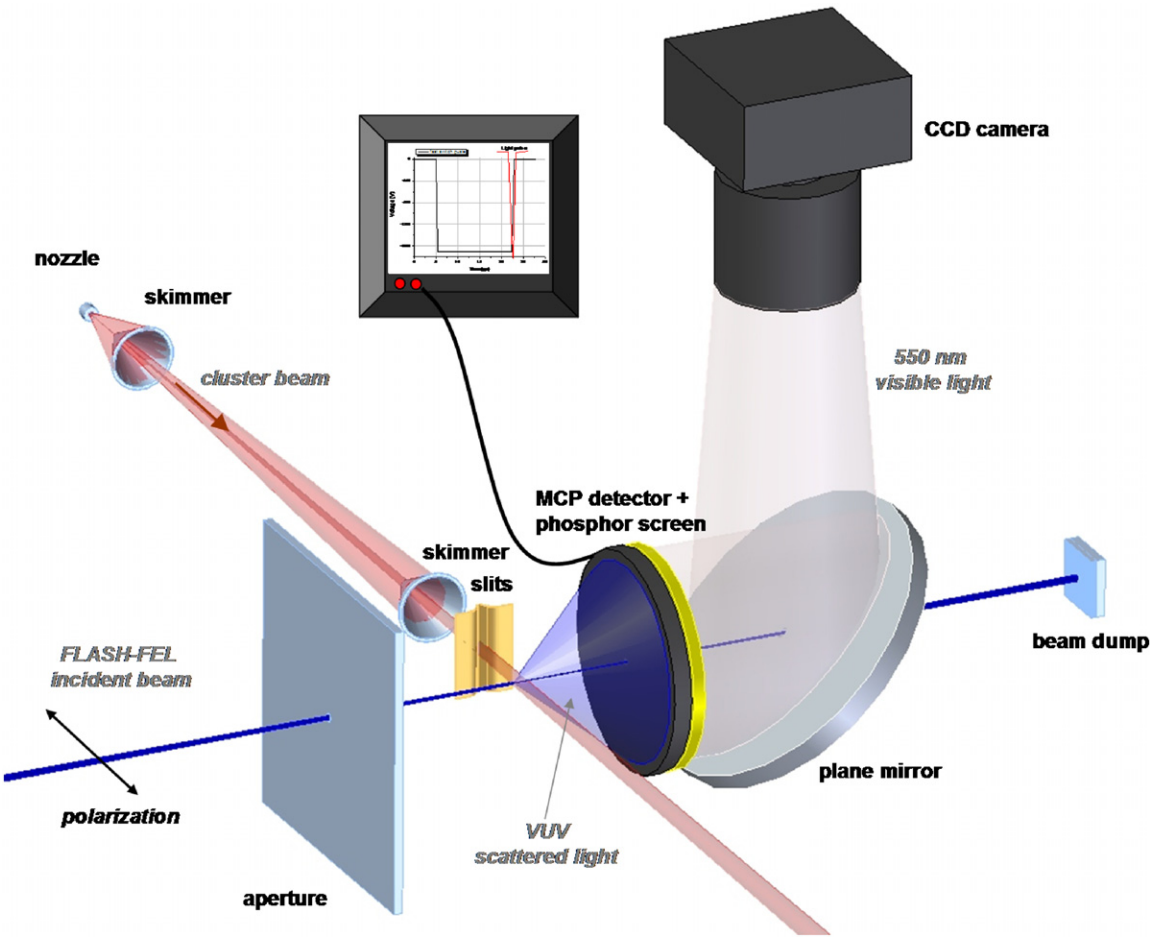

Figure 1. Schematic illustration of the imaging detector for recording of scattering patterns of clusters.

a power density up to 10^{13} W cm^{-2}. The energy of one photon was larger than the ionization potential of Xe atoms and as a result cluster ionization with a single photon became possible, in contrast to earlier work with intense IR and optical light pulses. The power density of the first FLASH experiments was sufficient to saturate the single-photon absorption. Figure 2 shows a comparison of the tof mass spectra of Xe atoms and clusters recorded at 8×10^{12} W cm^{-2}. For the largest cluster, several broad peaks can be seen which are due to singly and multiply charged Xe atoms. The most striking result is the different ion signal from atomic and cluster beams [3]. While only singly charged ions are observed after irradiation of atoms, ions with charges up to 8^+ are detected if clusters are irradiated. Doubly charged ions resulting from the ionization of isolated Xe atoms are not detected, at least under these conditions. Clusters absorb many photons per atom and completely disintegrate into singly and multiply charged ions. Larger cluster fragments could not be detected. The mass peaks are very broad, indicating that the ions carry high kinetic energy. This can be understood in terms of a Coulomb explosion process. The population of different ion states and their kinetic energies strongly depends on the power density [3]. This strong dependence on the power density is a clear sign that optical nonlinear processes dominate the ionization of the clusters at the power levels used. Similar results were found for Ar clusters [20]. If the power density is increased from 1×10^{11} W cm^{-2} to 2×10^{13} W cm^{-2} the mean charge state increases from 1 to ~3. At the time the experiment was performed, the strong absorption Xe clusters (the absorption *per atom* in the cluster), especially in comparison with isolated Xe atoms came as a surprise. In contrast to the work in the IR spectral range, the effect of the radiation *field* on the cluster is expected to be small. The ponderomotive energy, which is essentially the average kinetic energy of an electron oscillating in the presence of the intense light field, is in the meV regime since it scales with λ^2. For comparison, under standard high field conditions in the IR regime it is typically 10–100 eV thus exceeding the ionization potential of the cluster atoms. Shortly after publication of the experimental results, several theoretical models have been proposed to explain the efficient absorption in clusters [21–25]. In essence, under the special conditions of this experiment with photon energies just above the ionization potential a nanoplasma is formed which becomes temporarily strongly coupled. The efficient heating is due to IBS; however, the absorption and ionization processes differ from that in IR-laser-produced plasmas and involve complicated many-body dynamics. The formation of Xe^{2+} by single-photon absorption becomes possible in the plasma through barrier suppression which is prohibited in the isolated atom at this energy. Then, the plasma undergoes IBS heating. High charge states are formed through collisional

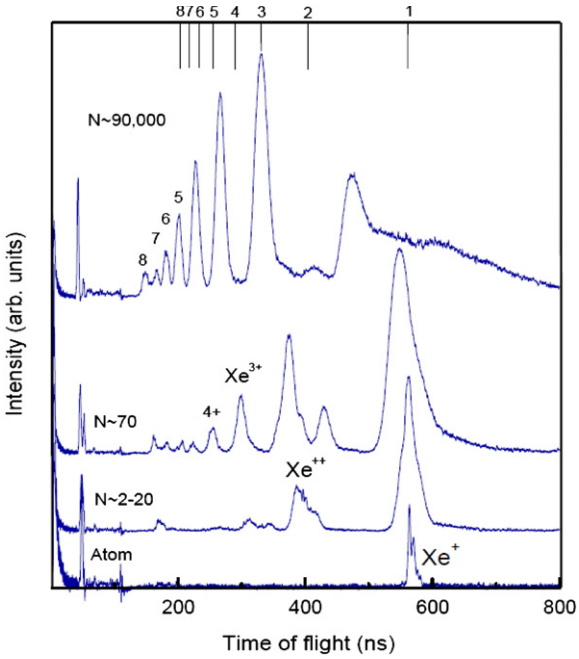

Figure 2. Time-of-flight mass spectra of ionization products of Xe atoms and clusters recorded following irradiation with 98 nm wavelength at a power density of 8×10^{12} W cm^{-2}. The mean cluster size and the different charge states are indicated in the figure. Please note that the power density was recalibrated after publication [3].

ionization and recombination of free electrons into excited states which undergo subsequent reionization. The cluster becomes charged as energetic electrons evaporate from its surface (*outer* ionization). During this process, the cluster potential gets very steep. Finally, the cluster expands due to the pressure of the electron gas and the cluster's own charge (Coulomb explosion). This process is illustrated in figure 3. The theoretical descriptions are summarized in recent papers [7, 25, 26].

Subsequent experiments at shorter wavelength clearly above the ionization potential made immediately clear that the role of plasma heating by inverse bremstrahlung becomes less and less important with increasing photon energy (see also section 3.2). Argon clusters irradiated with 32 nm FEL pulses and power densities of 4×10^{14} W cm^{-2} exhibit ion kinetic energies of a few eV only and larger cluster fragments appear [10], similar to the subsequent experiments at 51 nm [27]. At shorter wavelength, when inner-shell electrons can be excited, the cluster ionization becomes strongly dependent on the photoionization cross section. In figure 4, a comparison of the ion spectra of Xe, Ar and Kr clusters irradiated by 90 eV photons is presented. At this short wavelength the main products are singly charged ions, in contrast to results in the VUV spectral range at 12.7 eV where highly charged ions are rather prominent. In an atomic beam, highly charged ions are quite pronounced under the same conditions [11, 28]. This can also directly be seen in figure 4, especially for Xe where the sharp lines are due to highly charged ions from the uncondensed gas. The broad peaks are due to ions from clusters carrying kinetic energy up to a few hundred eV [12]. The intensity increases from Kr, Ar to Xe. This trend differs from the findings at lower photon energy, in particular in the IR regime. Usually Ar shows the weakest absorption and Xe the strongest, while Kr is intermediate. The trend for IR light results from the ordering of ionization potentials and polarization. The present results at 90 eV give direct evidence that here the absorption is linked to the single photoabsorption cross section at 90 eV. With 20 Mbarn Xe has by far the largest cross section which is due to excitation of 4d innershell electrons into the giant resonance peaking at 100 eV. The absorption cross section of Ar and Kr is considerably smaller, 1.5 Mbarn for Ar and 0.6 Mbarn for Kr. The cross section of Kr is rather small because 90 eV is very close to the energy of the minimum of the 4p $\rightarrow$ d continuum transition matrix element (Cooper minimum) [29].

More detailed insight into the charge redistribution and cluster explosion dynamics can be obtained from heterogeneous clusters, especially core–shell systems [11]. Such systems are also relevant for future (bio-) molecule tampers in imaging experiments [30]. In first experiments, Xe atoms in the core, surrounded by an Ar shell with variable thickness, are resonantly excited to high charge states. The m/q spectra for the core–shell systems are shown in figure 5. For the smaller systems $(N \approx 400)$ with a thin Ar coating,

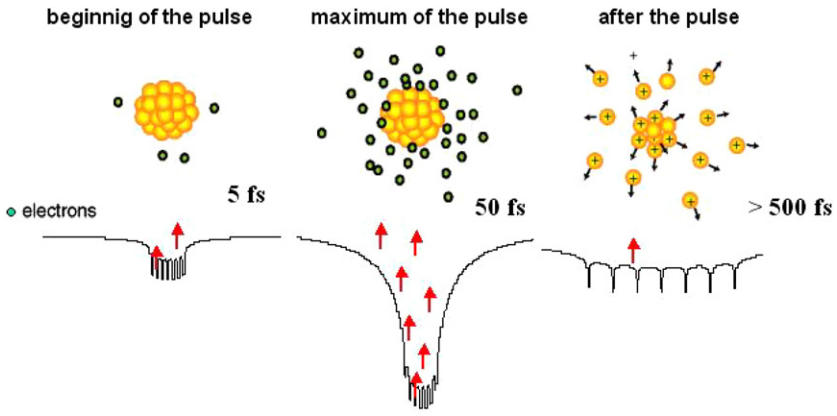

Figure 3. Schematic illustration of the ionization of Xe clusters and subsequent Coulomb explosion. The Coulomb potential of the clusters is shown at the beginning of the FEL pulse, at its maximum and at the end of the pulse. Photons are indicated by arrows.

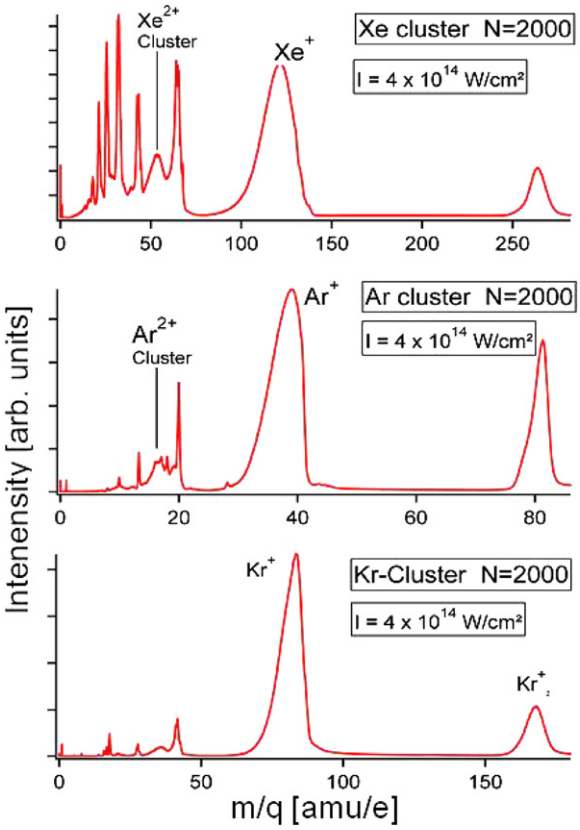

Figure 4. Time-of-flight mass spectra of ionization products of Xe, Ar and Kr clusters recorded following irradiation with 13.5 nm wavelength (corresponding to 90 eV) at a power density of 4×10^{14} W cm^{-2}. The mean cluster size and the different charge states are indicated in the figure.

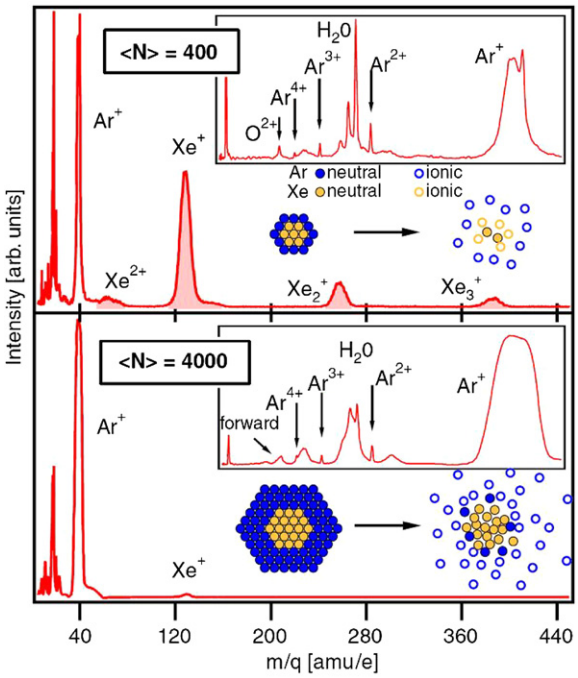

Figure 5. m/q spectrum of Xe core–Ar shell clusters with different sizes. Top: for small clusters ($N = 400$) predominantly the Xe cluster (filled) and Ar fragments are detected. Bottom: for large clusters ($N = 4000$) the Xe signal is virtually absent and the Ar signal including highly charged fragments becomes more intense. The insets depict the Xe distribution in the Ar cluster and the proposed expansion mechanism after irradiation. The arrows indicate the peak positions of high charge states [11].

the most intense signals stem from Xe fragments, namely Xe^+, Xe^{2+}, Xe^{3+} and the Ar^+ monomer. For $m/q < 40$ (inset in figure 5) predominantly higher Ar charge states and contributions from residual gas are present. Each Ar peak consists of a sharp main line from the atomic contribution and a shoulder on each side stemming from the cluster ions which are accelerated during the Coulomb explosion in or against the direction of the detector. Xe ions with charge states higher than 2, as seen in the case of atomic Xe and pure Xe clusters (compare figure 4), are not observed. The absence of highly charged Xe ions, while still the main absorption is due to Xe, shows that a fast charge redistribution from the multiply charged Xe to the surrounding Ar layers takes place. The spectra of the large Xe core–Ar shell clusters ($N \approx 4000$) with a thick Ar coating of about three or more shells look completely different (figure 5, bottom). The Xe signal is only 0.6% of the total signal, or in other words virtually absent, although the clusters contain $\sim 20\%$ Xe atoms. The dominant signal is now the Ar monomer with a significantly higher kinetic energy. Further, the multiply charged cluster Ar fragment signal becomes much more intense when compared with the smaller core–shell system (upper panel) or pristine Ar clusters (figure 4). The fact that only a very small amount of Xe^+ fragments can be detected indicates that efficient charge recombination processes take place because the fraction of Xe atoms in the cluster is much larger. Following the concept of *inner* and *outer* ionization [5], the Xe atoms in the core become multiply ionized through the FEL pulse [28]. Therefore the strong decrease in the Xe signal and increase in the Ar charge states and fragment kinetic energies for larger clusters must be caused by charge transfer, relaxation and separation dynamics, which are related to the size of the cluster and its shell structure. Considering the structure of the clusters, the detected Ar ions can only be ejected from the few outermost Ar surface layers, giving evidence of the Coulomb explosion of the cluster outer part only. The absence of the Xe signal in the m/q spectrum (figure 5, bottom) suggests that the highly charged Xe nanoplasma core recombines with quasi-free electrons and thus cannot be detected. The recombination of the nanoplasma core can be understood if the details of the cluster ionization are considered. At short wavelengths and the current power densities, the cluster ionization is largely due to photoemission in the building Coulomb potential [10]. Since the total energy needed to remove N electrons from a cluster with N atoms scales with $N^{5/3}$, the fraction of electrons which can escape drops significantly for larger clusters. Electrons that cannot overcome the Coulomb barrier lead to the formation of the nanoplasma, akin to *inner* ionization. These quasi-free photoelectrons thermalize and the plasma core can recombine. The nanoplasma charge imbalance is neutralized by exploding off the outermost cluster layers. Such a Coulomb explosion of the cluster outer layers and recombination of the nanoplasma core are also expected to take place in larger homogeneous clusters. However, it is much more difficult to detect because

the spatial origin of the charge states cannot be tracked with conventional tof mass spectroscopy as in the presently investigated core–shell systems. The findings are supported by theoretical work. Efficient recombination in the cluster core has been suggested to explain differences in observed and calculated charge states [23]. Further, recent theoretical work predicts that such charge redistribution and neutralization processes will turn the cluster Coulomb explosion into a much slower (>ps) hydrodynamic expansion [25, 31, 32]. The presence of a neutral core inside highly ionized clusters is also supported by a recent study of Xe clusters irradiated by 90 eV photons [12]. Here, the simulation of the measured kinetic energies suggests that highly charged ions explode off the surface due to Coulomb explosion while the inner core expands in a hydrodynamic expansion. The simulation, based on a simple electrostatic model, also gave evidence for an efficient ionization process of the cluster in addition to the direct multistep photoemission [10] which will be described in the next section.

3.2. Electron dynamics and energy transfer process studied with electron spectroscopy

From the discussion in the preceding section, it is evident that the electron and ion dynamics of clusters exposed to intense short-wavelength pulses are highly time-dependent processes. During the interaction with the light pulse, electrons are removed from the individual atoms (*inner* ionization) but only the first few photoelectrons, granted they have sufficient kinetic energy Auger electrons, can escape the cluster Coulomb potential. Ion spectroscopy can yield detailed information on the photoabsorption processes and to some extent also on the total energy absorbed. With electron spectroscopy, on the other hand, complementary information on the energy flow and deep insight into the energy exchange processes can be obtained. Photoemission gives a fingerprint of the electronic structure, in particular if applied with short-wavelength radiation [33]. In the first photoemission study of clusters at FLASH, Xe and Ar clusters were irradiated with 13 eV photons [34]. Here, the photon energy is only slightly larger than the Xe ionization potential but it is still smaller than the ionization potential of Ar. Thus, photoionization of Ar clusters can only be accomplished by two-photon processes. Since the photon energy is just 0.8 eV larger than the ionization of Xe, electrons emitted from atomic Xe are close to threshold forming a low-energy peak below 1 eV [34]. The electron spectrum of clusters recorded at the same conditions with a power density of 5×10^{12} W cm^{-2} also exhibits low kinetic energy with an almost thermal distribution and energies up to 30 eV. Since the ionization potential of the cluster increases with the emission of every electron, only a few electrons can be directly emitted. On the other hand, as discussed in the preceding section, at 13 eV the clusters are efficiently heated by IBS. The energy absorbed through the process of IBS exceeds that due to photoionization by more than a factor of 5 [26]. Therefore the electrons gain substantial energy, allowing them to be evaporated from the cluster surface in a thermal process [34]. This picture is supported by recent theoretical work [35].

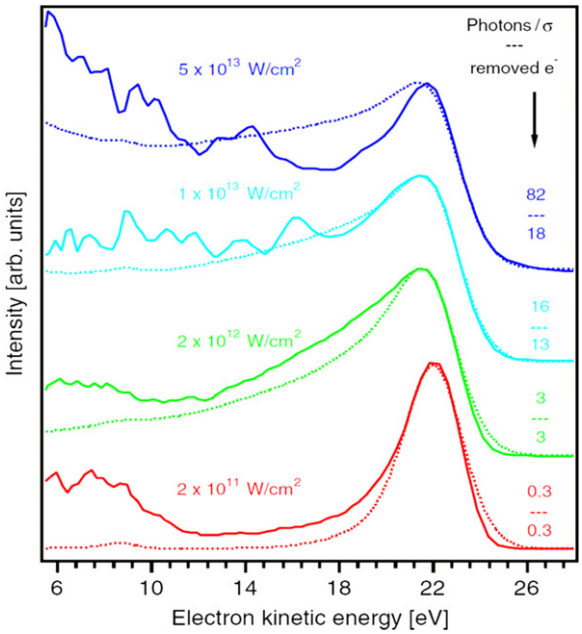

Figure 6. Experimental (solid line) and modelled (dashed line) electron spectra for Ar_{80} clusters for increasing power densities from bottom to top. The numbers on the right-hand side indicate how many photons fall into the absorption cross section of the cluster and how many electrons can overcome the increasing Coulomb barrier [10].

By going to higher photon energy, the scenario changes substantially as heating by IBS becomes insignificant [10]. For laser intensities up to 5×10^{13} W cm^{-2} and a photon energy of 37.8 eV, the cluster ionization process is a sequence of direct electron emission events in a developing Coulomb field. A nanoplasma is formed only at the highest investigated power densities where ionization is frustrated due to the deep cluster potential [10]. This conclusion is drawn from electron spectra presented in figure 6 and Monte Carlo simulations in figure 7. The electron spectra of Ar clusters comprising on average 80 atoms show a pronounced peak at 22 eV and a tail to lower energies which gains intensity with increasing power density. A pronounced wing towards high kinetic energies, a characteristic for thermionic electron emission as discussed above, cannot be observed. The main feature at 22 eV is due to the emission of the first photoelectron and can thus be assigned to the Ar 3p main line. The second photoelectron experiences already an increased charge in the cluster and is shifted accordingly to lower energies. At high power densities, this process continuous until the electrons do not have sufficient energy to escape from the increasingly deep cluster potential and the photoionization becomes frustrated. A quantitative description of the electron emission with Monte Carlo simulations is presented in figure 7. Here, the averaged spectra of individual electrons following consecutive absorption of photons are given. The broadening of the single-electron spectra is due to different position of the positively charged holes in the cluster. The sum spectrum exhibits a shape similar to the experimental spectra in figure 6, which also shows modelled spectra for different power densities. At the highest power density ($5 \times$

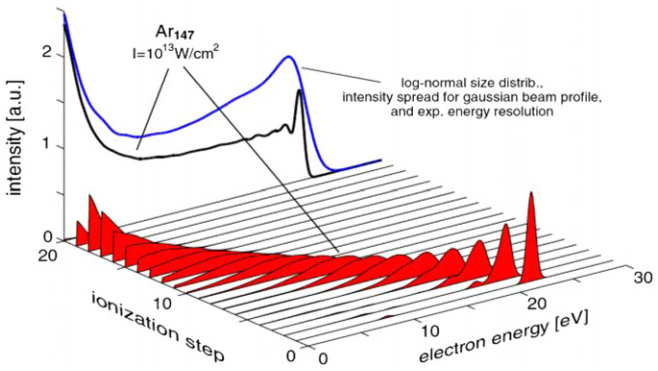

Figure 7. Monte Carlo simulations of the electron emission from an Ar_{147} cluster (see the text). The averaged spectra of each emitted electron numbers (filled graphs) as well as their average (black line) are shown. For comparison with the data, the relevant broadening effects are considered [10].

10^{13} W cm^{-2}), only 20% of the primary electrons released by photoemission from the individual cluster atoms can overcome the increasing Coulomb barrier [10]. The good agreement between experimental results and simulation and the absence of a 'thermionic' electron continuum gives evidence that IBS is insignificant at this energy (37.5 eV) and a power density up to 10^{14} W cm^{-2}. Similar results have been obtained in subsequent experiments for wavelength around 60 nm [36] even though IBS heating can in principle contribute for very long pulses at this wavelength [37].

We have already pointed out that the giant resonance of Xe which is due to 4d innershell ionization results in a large photoabsorption cross section at 90 eV. The ion spectra (figure 4) and the simulation of the kinetic energies in a simple electrostatic model [12] gave evidence that the direct multistep photoemission cannot solely account for the large kinetic energies seen in those experiments [12]. The amount of charges on the cluster needed to model the measured ejection energies of ions is 3–5 times larger than the number of electrons that can leave the cluster before the multistep ionization becomes frustrated. Here, electron spectroscopy in combination with simulations of the time-dependent electron dynamics can help to identify an additional ionization process. Figure 8 displays electron distributions of Xe clusters with a mean size of 2000 atoms for different intensities spanning a range from below 1.0×10^{13} W cm^{-2} to 5.8×10^{14} W cm^{-2}. At the lowest investigated intensity of 1.0×10^{13} W cm^{-2}, the photoelectron spectrum shows the pronounced peak of the 4d photoelectrons at around 22 eV and the Auger electrons around 32 eV. In addition, continua can be seen between both lines and below the 4d photo line. At the lowest intensity, the photoelectron spectrum of the cluster can still be understood in the picture of the multistep model [10]. For all spectra recorded at higher intensities, an additional signal above the 4d line eV appears which increases in intensity with respect to the 4d photoline as a function of power density. It becomes most prominent at the highest power density of about 5.8×10^{14} W cm^{-2}. This continuous signal stems from the 4d photoelectrons which, trapped in the strong Coulomb potential of the cluster ions, form a plasma

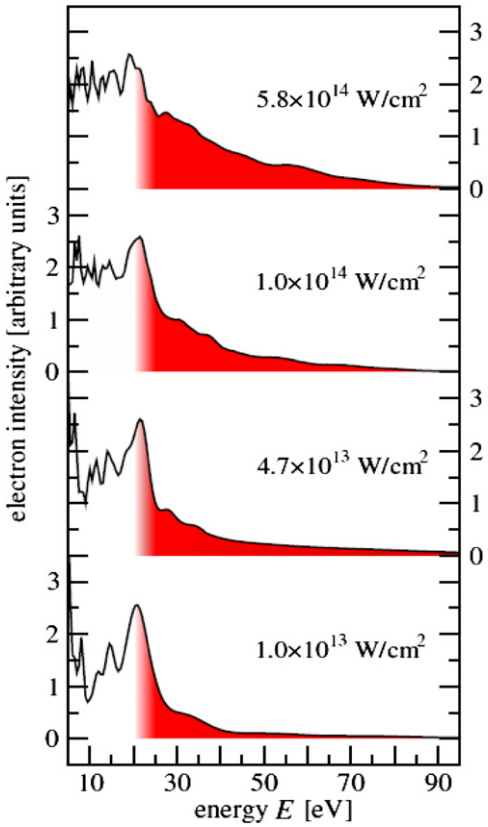

Figure 8. Electron spectra from Xe_N clusters with $N = 2000$ exposed to 10 fs FLASH pulses at 90 eV for various intensities. The line at 22 eV is due to the Xe 4d direct photoline. The shaded area marks electrons with energies higher than the photo line [38].

with supra-atomic density and which undergo multiple energy-exchanging collisions in the entire cluster volume producing an electron energy distribution with a tail of fast electrons [38]. The process differs from that described in the first part of this section. At 13 eV, all electrons are heated by IBS and accordingly they can overcome the Coulomb barrier in a highly charged cluster. In the case of 4d innershell ionization with a large single photoabsorption cross section, all electrons liberated from individual cluster atoms are energetically below the Coulomb barrier, once direct photoemission becomes frustrated. However, some of them can gain substantial kinetic energy by multiple energy exchanging collisions which allows them to leave the cluster [38]. Such collisional autoionization is expected to be a general phenomenon occurring for strong atomic x-ray absorption in extended systems.

3.3. Imaging of clusters and ultrafast processes probed with scattering techniques

One of the most fascinating prospects of research with intense short-wavelength FEL pulses is imaging of single nanoparticles. The key idea is the detection of sufficient scattered photons from an object before it is destroyed in the strong light pulse [39, 40]. Here, we present scattering patterns of single or a few clusters in the gas phase. The high intensity of the light pulses allows recording scattering patterns

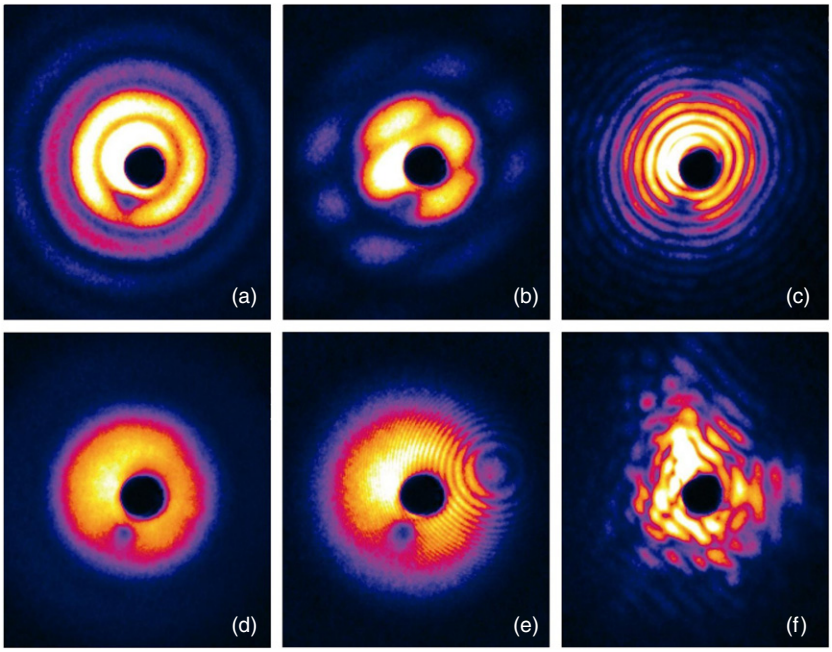

Figure 9. Single-shot scattering patterns of large Xe clusters. The patterns are recorded with the detector shown in figure 1: (a) a single cluster; (b) two clusters in direct contact; (c) a single large cluster; (d) an ensemble of many clusters (more than 10) in the focus; (e) two clusters separated by a large distance; (f) a complex pattern from en ensemble with unknown geometry.

in a single shot. Details will be given in the forthcoming publications [41, 42].

Figure 9 shows six single snapshots (out of thousands of similar pictures) recorded in single shots with 13 nm wavelength. The scattering patterns of single clusters (a), (c), or few clusters (b), (e) exhibit a wealth of details in contrast to featureless, smooth scattering patterns of a large ensemble of clusters (see figure 9(d)). However, these patterns, similar to diffraction patterns from a set of apertures in a flat screen, carry three-dimensional geometrical information and depend on the cluster dielectric function **n**. As we will see, they can be rather well understood in the framework of classical elastic scattering of light, e.g. *Mie scattering* [43].

Using simple scattering models, it can be concluded that images (a) and (c) with ring patterns come from single spherical clusters of increasing sizes. Patterns (b) and (e) with stripes and fine rings both come from two clusters, but with very different geometries: (b) indicates a dumbbell geometry with the axis orthogonal to the direction of the light beam, while (e) indicates two clusters, each cluster about the size of the cluster in image (b), but separated from each other by a much longer axis tilted with respect to the direction of the light beam. The pattern (e) exhibits some fine ring-type structure similar to Newton rings. The 'type (f)' image is due to a more complex geometry. The separation of the rings (figures 9(a) and (c)) is inversely proportional to the cluster diameter. Obviously, the total intensity of the scattering pattern increases with particle size. Under the present conditions, scattering pattern from clusters in the size range 20–300 nm radius could be recorded.

The experimental scattering patterns can be explained in the basis of scattering theory. Mie scattering refers to light scattering from homogeneous spheres with an arbitrary value for the complex dielectric constant **n**. The angular profile is obtained from a complete solution of Maxwell's equations of electrodynamics for the electric **E** and magnetic **B** fields in the presence of a dielectric sphere. Further, for explaining the scattering patterns, '*scalar models*' can be used [44]. They refer to light scattering from a set of pointlike independent scatterers, and apply to bodies of arbitrary shape and composition, but for them light absorption and multiple scattering are neglected. There is a rather wide range of parameters where both *Mie scattering* and *scalar models* are applicable to large Xe clusters and predict very similar angular patterns.

Figure 10 shows a more detailed comparison between a 'type (b)' single-shot experimental image from figure 9 and a simulation based on scalar theory for the angular distribution of light scattered by a dumbbell shaped or twin cluster with the same size. In contrast to a single spherical cluster, the scattering pattern shows pronounced stripes. The stripes, as in a double slit scattering experiment, give evidence that we have two scattering centres separated by some distance. The spacing of the stripes is a measure of the particle separation d and, if the particles are in a plane parallel to the detector, it is directly proportional to $1/d$. The shape of the interference stripes in the scattering pattern yields information about the orientation of the dumbbell structure in space. In figure 11, simulations for two clusters with identical size but different orientation with respect to the incoming photon beam are presented. It should be noted that the twinned clusters, a geometry that strongly departs from spherical, were not expected to be produced by a gas expansion cluster source. With the help of the simulated pattern in the right part of figure 10, we can conclude that the particles are 70 nm in diameter and in direct contact. Such information on

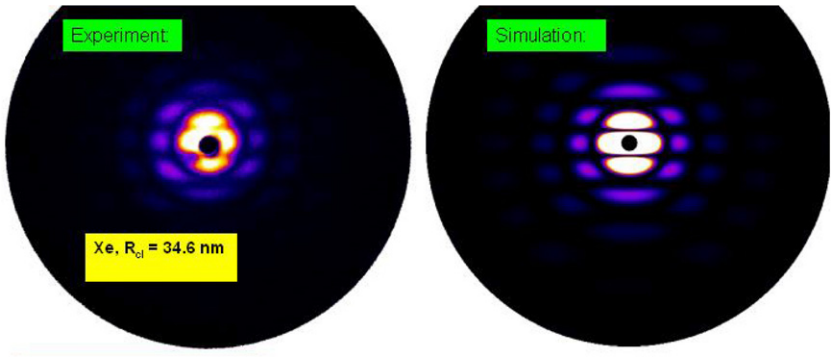

Figure 10. Detailed comparison between left: a single-shot experimental image (type 'b' from figure 9) and right: a simulation based on scalar theory for the angular distribution of light scattered by a dumbbell shaped or twin cluster with the same size.

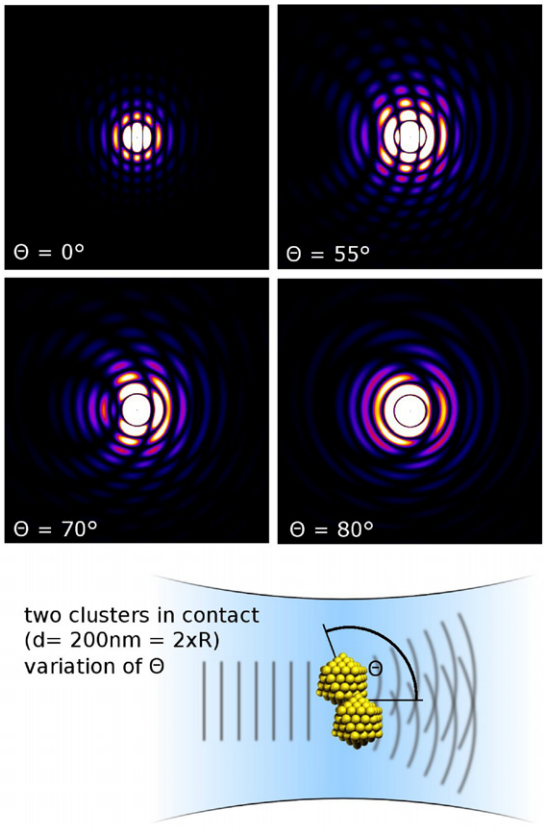

Figure 11. Simulations for two clusters with identical size but different orientation with respect to the incoming photon beam.

clusters cannot be obtained with mass spectroscopy or any spectroscopic technique. Moreover, the presence of a large number of twinned clusters in beam—of the order of 1%—produced by an adiabatic expansion of a cold gas came as quite a surprise.

The scattering pattern in figure 9(e), which exhibits strong similarities with Newton rings, can be explained in a similar way by numerical simulation [45]. In this case, the two-dimensional scattering patterns give information about the three-dimensional configuration of two clusters, which are separated by a few microns. The observed Newton ring-type scattering patterns result from a coherent superposition of two spherical waves. The line connecting the two clusters points into the direction of the central maximum of the Newton ring. The separation of the rings decreases with the square root of the separation from the centre of the ring, and it contains the information on the particle separation parallel to the FEL beam. Details will be discussed in a forthcoming publication [42]. In this way, three-dimensional structural information can be obtained from two-dimensional scattering data. Simulations similar to that shown in figure 10 (right) and figure 11 for different distances can give direct insight how the 'stripes' develop into 'Newton rings' when the angle and the separation are varied [42]. The curvature of the rings (see figure 11), and especially the asymmetry, contains information about the angle between the clusters with respect to the incoming photon beam while the spacing of the rings is a measure of their separation. Such information can also be obtained with Fourier transform techniques [40] applied to the experimental image, as pointed out very recently with a new approach [46]. Here we report on simple first results for a 'real sample' instead of a test object. In the present case, the separation of the two clusters in figure 9(e) of 2.8 μm is derived with the simulations [42].

With upcoming hard x-ray sources, these imaging experiments offer exciting prospects such as direct imaging of clusters and other nonperiodic nanoscale objects with a resolution reaching the atomic level. Unprecedented details of the cluster structure can then be revealed. The ongoing research is an important step towards this goal.

4. Conclusion and outlook

Clusters in intense soft x-ray pulses exhibit interesting, highly time-dependent ionization dynamics. The first experiments in this field were performed with power densities up to 10^{15} W cm^{-2}. The data show that absorption and ionization processes in the high power-density regime are strongly wavelength dependent. While at the lowest energies in the spectral range around 10 eV plasma absorption by IBS is the dominant heating process, it becomes less and less important with increasing photon energy. At energies above 40 eV and power densities up 10^{13} W cm^{-2}, the cluster ionization is best described by multistep photoionization, which becomes frustrated in the increasing Coulomb potential. This process is governed by the single-photon absorption cross section and takes place on the few fs timescale during the pulse. At the

highest investigated power densities, nanoplasmas with supra-atomic density are created and energy-exchanging electron collisions can lead to further cluster ionization. The ion spectroscopy data give evidence that although the clusters are getting highly charged, an almost neutral plasma is formed in the cluster core due to nanoplasma recombination. With scattering techniques, snapshots of single clusters can be recorded with single soft x-ray light pulses. The scattering patterns provide information on the two-dimensional as well as three-dimensional structure of clusters and of cluster ensembles. Meanwhile, time-resolved experiments with pump–probe techniques have started which allow following the time evolution of cluster ionization up to several ps. With even shorter wavelength, now already available at the LCLS, ionization processes involving core levels can be addressed and clusters are imaged with nanometre resolution.

Acknowledgments

We would like to thank the DESY staff for their outstanding support and our colleagues from Universität Rostock, MPI-PKS, MPG-ASG, MPI-K, MPG-HLL, DESY and Amolf for inspiring and fruitful collaborations. Funding is acknowledged from BMBF grant no 05KS4KTC1, DFG BO 3169/2-2 and HGF Virtuelles Institut VHVI-302.

References

[1] Ackermann W *et al* 2007 Operation of a free-electron laser from the extreme ultraviolet to the water window *Nat. Photonics* **1** 336
[2] Bostedt C *et al* 2009 Experiments at FLASH *Nucl. Instrum. Methods Phys. Res.* A **601** 108–22
[3] Wabnitz H *et al* 2002 Multiple ionization of atom clusters by intense soft x-rays from a free electron laser *Nature* **420** 482–5
[4] Ditmire T *et al* 1996 Interaction of intense pulses with atomic clusters *Phys. Rev.* A **53** 3379–402
[5] Last I and Jortner J 2000 Dynamics of the Coulomb explosion of large clusters in a strong laser field *Phys. Rev.* A **62** 13201 1–9
[6] Last I and Jortner J 1999 Quasiresonance ionization of large multicharged clusters in a strong laser field *Phys. Rev.* A **60** 2215–21
[7] Saalmann U, Siedschlag C and Rost J M 2006 Mechanisms of cluster ionization in strong laser pulses *J. Phys. B: At. Mol. Opt. Phys.* **39** R39–97
[8] Krainov V P and Smirnov M B 2002 Cluster beams in superintense femtosecond laser pulse *Phys. Rep.* **370** 237–331
[9] Krainov V P 2000 Inverse stimulated bremsstrahlung of slow electrons under Coulomb scattering *J. Phys. B: At. Mol. Opt. Phys.* **33** 1585–95
[10] Bostedt C *et al* 2008 Multistep ionization of argon clusters in intense femtosecond extreme ultraviolet pulses *Phys. Rev. Lett.* **100** 133401
[11] Hoener M *et al* 2008 Charge recombination in soft x-ray laser produced nanoplasmas *J. Phys. B: At. Mol. Opt. Phys.* **41** 181001
[12] Thomas H *et al* 2009 Shell explosion and core expansion of xenon clusters irradiated with intense femtosecond soft x-ray pulses *J. Phys. B: At. Mol. Opt. Phys.* **42** 134018
[13] Mitzner R *et al* 2009 Direct autocorrelation of soft-x-ray free-electron-laser pulses by time-resolved two-photon double ionization of He *Phys. Rev.* A **80** 025402
[14] Tiedtke K *et al* 2009 The soft x-ray free-electron laser FLASH at DESY: beamlines, diagnostics and end-stations *New J. Phys.* **11** 023029
[15] Buck U and Krohne R 1996 Cluster size determination from diffractive He atom scattering *J. Chem. Phys.* **105** 5408
[16] Karnbach R *et al* 1993 CLULU: an experimental setup for luminescence measurements on van der Waals clusters with synchrotron radiation *Rev. Sci. Instrum.* **64** 2838–49
[17] Lengen M *et al* 1992 Site-specific excitation and decay processes in XeAr clusters *Phys. Rev. Lett.* **68** 2362
[18] Laarmann T *et al* 2002 Tightly bound excitons in small argon clusters: insights from size-dependent energy shifts *Phys. Rev.* B **66** 205407
[19] Danylchenko O G *et al* 2006 *JETP Lett.* **84** 324
[20] Laarmann T *et al* 2004 Interaction of argon clusters with intense VUV-laser radiation: the role of electronic structure in the energy-deposition process *Phys. Rev. Lett.* **92** 143401
[21] Santra R and Green C 2003 Xenon clusters in intense VUV laser fields *Phys. Rev. Lett.* **91** 233401
[22] Bauer G 2004 Small rare gas clusters in laser fields: ionization and absorption at long and short laser wavelength *J. Phys. B: At. Mol. Opt. Phys.* **37** 3085–101
[23] Siedschlag C and Rost J M 2004 Small rare gas clusters in soft x-ray pulses *Phys. Rev. Lett.* **93** 43402
[24] Jungreuthmayer C *et al* 2005 Intense VUV laser cluster interaction in the strong coupling regime *J. Phys. B: At. Mol. Opt. Phys.* **38** 3029–36
[25] Ziaja B *et al* 2009 Energetics, ionization, and expansion dynamics of atomic clusters irradiated with short intense vacuum-ultraviolet pulses *Phys. Rev. Lett.* **102** 205002
[26] Walters Z B, Santra R and Greene C H 2006 Interaction of intense VUV radiation with large xenon clusters *Phys. Rev.* A **74** 043204
[27] Fukuzawa H *et al* 2009 Dead-time-free ion momentum spectroscopy of multiple ionization of Xe clusters irradiated by EUV free-electron laser pulses *Phys. Rev.* A **79** 031201
[28] Richter M *et al* 2009 Extreme ultraviolet laser excites atomic giant resonance *Phys. Rev. Lett.* **102** 163002
[29] Cooper J W 1962 Photoionization from outer atomic subshells: a model study *Phys. Rev.* **128** 681 LP–693
[30] Hau-Riege S P *et al* 2007 Encapsulation and diffraction-pattern-correction methods to reduce the effect of damage in x-ray diffraction imaging of single biological molecules *Phys. Rev. Lett.* **98** 198302
[31] Rusek M and Orlowski A 2005 Different mechanisms of cluster explosion within a unified smooth particle hydrodynamics Thomas–Fermi approach: optical and short-wavelength regimes compared *Phys. Rev.* A **71** 043202
[32] Ziaja B *et al* 2008 Femtosecond non-equilibrium dynamics of clusters irradiated with short intense VUV pulses *New J. Phys.* **10** 043003
[33] Siegbahn K *et al* 1969 *ESCA Applied to Free Molecules* (Amsterdam: North-Holland)
[34] Laarmann T *et al* 2005 Emission of thermally activated electrons from rare gas clusters irradiated with intense VUV light form a free electron laser *Phys. Rev. Lett.* **95** 63402
[35] Ziaja B *et al* 2009 Emission of electrons from rare gas clusters after irradiation with intense VUV pulses of wavelength 100 nm and 32 nm *New J. Phys.* **11** 103012
[36] Iwayama H *et al* 2009 Frustration of direct photoionization of Ar clusters in intense extreme ultraviolet pulses from a free electron laser *J. Phys. B: At. Mol. Opt. Phys.* **42** 134019

[37] Georgescu I, Saalmann U and Rost J M 2007 Clusters under strong VUV pulses: a quantum-classical hybrid description incorporating plasma effects *Phys. Rev.* A **76** 043203
[38] Bostedt C *et al* 2010 Fast electrons from multi-electron dynamics in xenon clusters induced by inner-shell ionization *New J. Phys.* **12** 083004
[39] Neutze R *et al* 2000 Potential for biomolecular imaging with femtoscond x-ray pulses *Nature* **406** 752–7
[40] Chapman H N *et al* 2006 Femtosecond diffractive imaging with a soft-x-ray free-electron laser *Nat. Phys.* **2** 839–43
[41] Bostedt C *et al* 2010 Ultrafast scattering as a probe for transient states of matter to be published
[42] Rupp D *et al* 2010 to be published
[43] Born M and Wolf E 2002 *Principle of Optics* (Cambridge: Cambridge University Press)
[44] de Castro A R B *et al* 2008 Numerical simulation of small angle scattering (SAXS) for large atomic clusters *J. Electron Spectrosc. Relat. Phenom.* **166** 21–7
[45] Rupp D 2008 *Simulation und Auswertung von Streuexperimenten am FEL für weiche Röntgenstrahlung* (Berlin: TU-Berlin)
[46] Raines K S *et al* Three-dimensional structure determination from a single view *Nature* **463** 214–7